Journal of the Serbian Chemical Society
JSCS-info@shd.org.rs • www.shd.org.rs/JSCS
J. Serb. Chem. Soc. *81* (7) 763–776 (2016) UDC 547.861–327:548.33:548.7:536.7:541.121
JSCS–4884 *Original scientific paper*

Ab initio prediction of the polymorphic structures of pyrazinamide – A validation study

DAVID STEPHEN ARPUTHARA[1]*, PALLIPURATH VELEELATH NIDHIN[1] and PONNUSAMY SRINIVASAN[2]

[1]*Department of Physics, Sri Shakthi Institute of Engineering and Technology, Coimbatore, India;* [2]*Department of Physics, C. Kandaswami Naidu College for Men, Anna Nagar, Chennai, India*

(Received 10 December, revised 15 March, accepted 7 April 2016)

Abstract: A validation study to predict the possible stable polymorphs of pyrazinamide within the low energy conformational region of the flexible torsion angle was performed through a potential energy surface (PES) scan by gas phase optimisation using the MP2/6-31G(d,p) method. Hypothetical crystal structures with favourable packing density for each of the stable conformers generated from the PES scan were generated using a global search with a repulsion only potential field. The densest crystal structures with stable energy were analyzed with more accurate lattice energy minimisation *via* distributed multipole analysis using the repulsion–dispersion potential. The stability of the predicted crystal structures with similar close packing to the known experimental polymorphs of the pyrazinamide molecule were analyzed by inspecting their intermolecular short contacts. Studies to analyze the second derivative mechanical properties from the Hessian matrix were realised to emphasise the thermodynamic stability of predicted polymorphs of pyrazinamide.

Keywords: *Ab initio* crystal structure prediction; polymorphs; PES scan; lattice energy minimisation; Hirshfeld surface.

INTRODUCTION

Polymorphism is the property of a molecule that describes its ability to crystallise in more than one crystal form. Theoretical work to identify the polymorphs is a subject of great academic and industrial importance, since the experimental observation of certain polymorphs is sometimes very challenging. Polymorphic structures can have similar or very different chemical and physical properties from the parent structure,[1] which may alter, for example, their pharmaceutical effectiveness**.** Typical investigations to find the polymorphic landscapes are performed experimentally, but theoretical predictions can reduce the process

* Corresponding author. E-mail: davidstephen_dav@yahoo.co.in
doi: 10.2298/ JSC151210046D

time with much accuracy. As a result, techniques to predict crystal structures have been introduced and tested for various molecules. Recently, in a report on the fifth blind test, Price *et al.* analyzed the polymorphic hydrate gallic acid monohydrate[2] by refining the search space to a more manageable level by identifying the flexible torsions. Most of the crystal structure prediction (CSP) techniques assume that the stable polymorphs come in the lowest energy region of lattice-energy surface.[3]

Interesting and challenging tests for *ab initio* CSP techniques are the extent to which they can predict the polymorphs of the same crystal compositions. The current paper presents an attempt to predict the polymorphic structures of pyrazinamide, within a flexible torsion range and a specific potential field. Pyrazinamide is an antitubercular drug molecule, which can shorten the therapy to 6–9 months and has a better effect over semi-dormant bacilli.[4] The concerned pyrazinamide molecule has four known polymorphic forms, *α, β, γ* and *δ*.[5] The structural reports of these known polymorphs revealed that the two-dimensional sheet-like appearance of the *β* polymorph contributes to a herring bone motif, and similar can be observed for the *δ* polymorph; whereas the *α* and *δ* forms exist as simple sheet structures.[6] Detailed analysis of the intermolecular short contacts of the four polymorphic forms indicated the presence of a dimer interaction between the carboxylic and the amide functional group, which was absent for the *γ* polymorph. The presence of strong π···π stacking for the *γ* polymorph causes the crystal structure to create face–face stacks whereas an edge–face interaction was exhibited by the *δ* polymorph.[7] Studies of these structures showed that the known polymorphic forms arose from deviation in the short contacts and the hydrogen bond motifs that may affect the solubility of the pyrazinamide molecule, which in turn is one of the favourable qualities of a pharmaceutical compound. As explained, the presence of polymorphic structures may change the physical and chemical properties of molecules, and may alter their medicinal value. Thus the need for *ab initio* CSP techniques to predict the polymorphs of different organic molecules justifies its importance.

AB INITIO METHODOLOGY

The crystal structure prediction methodology for flexible molecules exhibiting conformational polymorphism should evaluate and compare the relative energy penalty for the intramolecular distortion of the molecule to verify its stability using Eq. (1):

$$E_{\text{total}} = U_{\text{lattice}} + \Delta E_{\text{intra}} \quad (1)$$

The commonly used *ab initio* CSP method starts with a potential energy surface scan with a flexible torsion angle and global search to identify the likely crystal structures within the crystal energy landscape. The selected best crystal structures were then subjected to lattice energy minimisation. The same methodology was used in the current paper with the potential energy surface scan executed using the MP2 method with the 6-31G(d,p*)* basis set in Gaussian 09.[8] A global MOLPAK[9] search for the densest hypothetical crystal structures within the

crystal energy landscape was realised by performing step-by-step orientations of the concerned molecule in all common coordination geometries for constructing the appropriate coordination patterns with the unit cell volume as the function to be minimised. The algorithm uses a repulsion only UMD potential to build the packing arrangements in the commonly encountered space groups P1, P 1 , P2, Pm, Pc, $P2_1$, P2/c, $P2_1$/m, P2/m, $P2_1$/c, Cc, C2, C2/c, Pnn2, Pba2, Pnc2, $P22_1$, $Pmn2_1$, Pma2, $P2_12_12_1$, $P2_12_12$, $Pca2_1$, $Pna2_1$, Pnma and Pbca. The densest hypothetical packings generated from the MOLPAK search were then subjected to more accurate lattice energy minimisation using DMACRYS,[10] which implements a repulsion–dispersion potential field of the form:

$$U = \Sigma_{i\in 1 k\in 2} [(A_{ii}A_{kk})^{1/2}]\exp[-(B_{ii} + B_{kk})R_{ik}/2] - (C_{ii}C_{kk})^{1/2}/R^6_{ik} \quad (2)$$

where i and k are the atoms in molecules 1 and 2 of different types. The parameters used in this study came from the FIT potential, parameterized by Williams and Cox,[11] with additional terms for the hydrogen atoms bound to nitrogen later fitted by Coombes *et al.*[12]

The thermodynamic stability of predicted crystal structures was verified from the second derivative properties from the DMACRYS optimization by confirming the Born stability criteria were met. The eigenvalues of the final optimized structure were evaluated for all the representations of the group to find the occurrence of any negative eigenvalues. The presence of negative eigenvalues indicates that the structure had been optimized to a saddle point between two lower symmetry structures. A valid minimisation can be performed in such cases by re-minimising the optimized structure after removing the corresponding representation of space group from the symmetry constraints to attain the true minimum.

In the next section, a detailed outline of the employed approach towards pyrazinamide is provided.

Potential energy surface scan with flexible torsion

The conformational diversity of a molecule increases with increasing number of flexible torsion angles,[13] and hence, the potential energy surface of flexible molecules which form different conformational structures should be analyzed.[14] The aim of this stage was to find the local minima of the low energy conformers within the energy landscape by performing a potential energy surface scan with a selected flexible torsion angle (θ), the variation of which plays a vital role in producing conformational polymorphism. A potential energy surface scan executed through a series of MP2 level gas phase optimizations gives detailed analysis of possible conformers of the molecule of interest and the energy barrier associated with the conformational changes of the flexible molecule and thereby locating local minima,[15] which is crucial for the prediction methodology.

The central aromatic ring of the pyrazinamide molecule was found to be rigid due to its π interactions compared to the terminal bonds. Since the range of conformers produced depends on the degrees of freedom of the flexible molecule, the terminal torsion angle N(3)–C(2)––C(1)–N(1) (θ) was selected as flexible for the current potential energy surface scan. Each point on the potential energy surface was considered to be a partial gas phase optimization with the MP2 level theory using the 6-31G(d,p) basis set, and varying θ from –180 to 180°. A plot of the energy difference of each conformer generated on the PES scan as the torsion angle varies from –180 to 180° with respect to the global minimum is shown in Fig. 1. The PES scan revealed that the conformer with lowest energy was attained at a torsion angle of 0° and is considered as the global minimum. The structural aspects of the conformers generated at the troughs of the PES scan were analyzed and studied thoroughly. The deep trough (at 0°) in the plot of the energy penalty against torsion angle (Fig. 1) arises from the geometric position of

the terminal nitrogen atom (N(1)] being *cis* to the ring nitrogen [N(3)), thereby enabling a strong intramolecular hydrogen bonding interaction. Two shallow troughs in the plot were found at the near *trans* position of N(1) and N(3) making a torsion angle of ≈140°. The stable conformers generated in the PES scan of the selected torsion angle were analyzed and those within an energy range of ≈10 kJ mol^{-1} of the global minimum[16] were selected for the MOLPAK global search. The selected conformers had the *cis* configuration of the key aromatic nitrogen with the terminal nitrogen atom, and a torsion angle ranging from –40 to 40°. All the other structures were not considered since they were found to be at higher regions of the energy plot and thus, it was very unlikely that the intermolecular energy could overcome the energy penalty for deformation of the molecule from the global minimum.

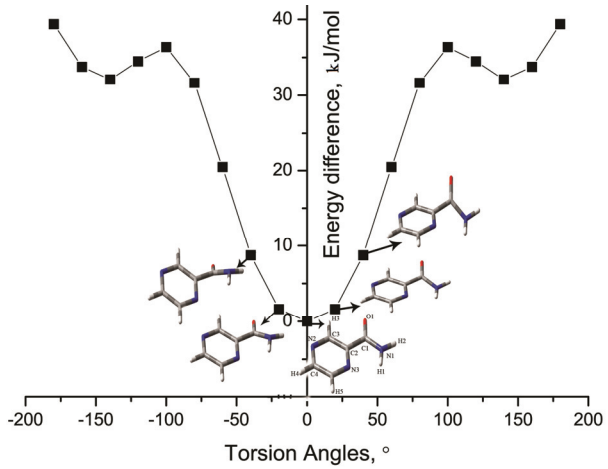

Fig. 1. Graph of energy difference *vs*. the torsion angle N(3)–C(2)–C(1)–N(1).

MOLPAK global search for the crystal structures

The prior background aim of the global search is to generate all the possible hypothetical dense structures with various space group symmetry within the lattice energy surface. All the generated structures within a specific space group were then optimized with the boundary values of decision variables like lattice lengths, lattice angles and Euler's coordinates which determine and specify the geometry of the unit cell. The optimized structures with calculated density less than the threshold density were taken as one of the possible crystal structures.

The global search for the crystal structures of pyrazinamide was realised using the MOLPAK algorithm, which reconstructs the optimized conformers on a three dimensional grid. All the unique orientations were obtained by rotation of the rigid molecule in 10° steps from –90 to 90° within the three Cartesian planes, generating 6859 (19^3) hypothetical starting molecules. Space group symmetry was then applied to generate the complete crystal structure. The packing density and the unit cell volume of each generated structure were analyzed with the PMIN refinement using a repulsion only UMD potential. The structures were ranked based on the packing density and the densest were carried forward to the lattice energy minimisation.[17] The current study of pyrazinamide dealt with the search in 25 commonly encountered space groups in the Cambridge Structural Database (CSD), from which about 1067 hypothetical crystal structures were selected as starting point for lattice energy minimisation.

DMACRYS lattice energy minimisation and selection of the final structures

The hypothetical densest rigid molecule crystal structures generated from the global search were selected as the starting points for the lattice energy minimisations to evaluate their thermodynamic stability using the DMACRYS algorithm, which incorporates a repulsion dispersion potential field of the form Eq. (2). The electrostatic and intramolecular interactions of the molecules were modelled through a set of atomic dipoles evaluated from a distributed multipole analysis of the MP2/6-31G(d,p) charge density using the GDMA algorithm.[18]

The DMACRYS lattice energy minimisation of the hypothetical rigid molecule crystal structures calculates the Ewald summed charge–charge, charge–dipole, dipole–dipole interactions[19] and the second derivative properties from the Hessian matrix to emphasise their stability and valid minimisation. The structures that had not reached true minima were at a transition state, which will reach true minima in further lattice minimisation within the interaction field. For pyrazinamide, it was noted that some of the crystal structures failed to reach true minima, generating non-zero eigenvalues for the coordination symmetry. Therefore repeated minimisation was done for such crystal structures to attain true minima, by removing the non-zero representation from the symmetry constraints.

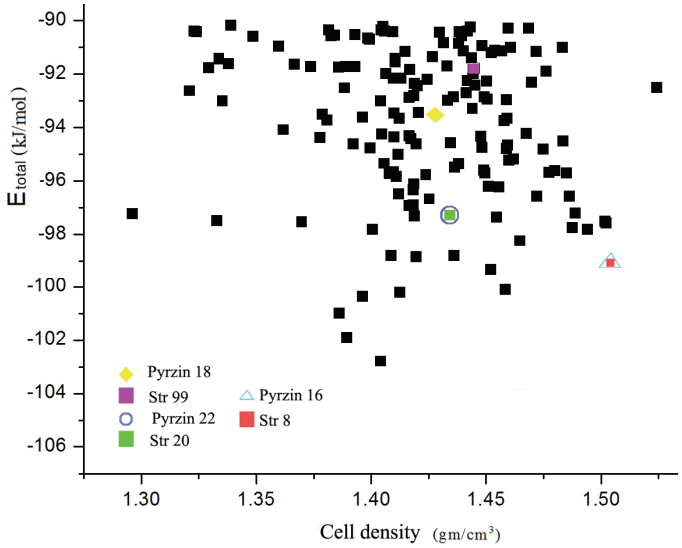

Fig. 2. The crystal energy landscape showing all the possible predicted stable crystal structures of the pyrazinamide molecule along with the minimised experimental pyrzin 16 (δ), pyrzin 22 (α) and pyrzin 18 (β) polymorphs.

Figure 2 shows the dense crystal energy landscape with the generated optimized crystal structures together with the minimised experimental pyrazinamide structure within the region from –90 to –103 kJ mol^{-1}. The predicted structures within this region are expected to be stable and crystallise under normal thermodynamic conditions. The densest crystal structures which are stable and match with the experimental crystal structures were evaluated from comparisons performed using COMPACK[20] with 20 molecules in the coordination sphere and 50 % tolerance to check the accuracy of the optimization technique and potential used.

RESULTS AND DISCUSSION

Analysis of the predicted conformers

The hypothetical crystal structures from the crystal energy landscape were sorted in increasing order of the total energy (E_{total}). The most stable structures from the landscape predicted *via* the *ab initio* crystal structure prediction method are presented in Table I. The structures that almost matched the experimental crystal were selected based on the root mean square deviation (*RMSD*) for the crystal packing similarity. The lowest energy optimized crystal structures could be considered as potential polymorphs of pyrazinamide.

TABLE I. List of lowest energy conformers identified *via ab initio* CSP together with the reproduced experimental polymorphs (δ, α and β) of pyrazinamide

Structure	Space group	a / Å	b / Å	c / Å	α / °	β / °	γ / °	$-U_{lattice}$ kJ mol^{-1}	$-E_{total}$ kJ mol^{-1}	Density g cm^{-3}
Str1	Pc	7.206	11.663	15.938	90.00	154.23	90.00	104.4143	102.803	1.4041
Str2	Pc	4.225	15.833	8.824	90.00	85.56	90.00	101.9214	101.921	1.3895
Str3	$P2_{111}$	6.345	15.916	11.685	90.00	90.00	90.00	102.6184	101.007	1.3861
Str4	$P2_1$	9.674	15.854	4.054	90.00	70.36	90.00	101.9925	100.381	1.3964
Str5	$Pna2_1$	8.870	15.491	4.213	90.00	90.00	90.00	100.2139	100.214	1.4126
Str6	$P2_1/c$	5.650	5.377	18.471	90.00	92.38	90.00	100.1129	100.113	1.4586
Str7	P1	5.797	6.624	7.563	89.89	85.02	76.74	99.3356	99.3356	1.4523
Str8	P1	5.852	6.356	13.152	53.75	130.69	129.85	100.6196	99.0078	1.504
Str9	P1	22.149	7.193	3.616	90.00	90.00	90.00	98.8418	98.8418	1.4196
Str10	C2/c	14.184	7.878	10.675	90.00	72.70	90.00	98.8156	98.8156	1.4361
Str11	P1	21.768	3.608	14.783	90.00	90.00	90.00	98.8047	98.8047	1.4088
Str12	$Pna2_1$	14.157	10.537	3.743	90.00	90.00	90.00	98.2558	98.2558	1.4648
Str13	$P2_1/c$	9.977	5.623	13.521	90.00	46.17	90.00	97.8271	97.8271	1.4943
Str14	P1	3.728	7.742	11.524	65.73	92.62	105.15	97.8262	97.8262	1.4006
Str15	P1	7.605	5.800	7.135	107.71	85.75	113.36	97.7639	97.7639	1.4878
Str16	$P2_1/c$	8.354	4.520	14.909	90.00	75.21	90.00	97.582	97.582	1.5023
Str17	$P2_12_12_1$	11.760	15.854	6.404	90.00	90.00	90.00	99.1534	97.5416	1.3699
Str18	$P2_1$	8.342	4.528	14.905	90.00	75.24	90.00	97.5236	97.5236	1.502
Str19	$P\bar{1}$	5.313	7.813	8.051	73.70	80.96	73.66	97.5112	97.5112	1.333
Str20	$P2_1/n$	3.658	6.898	22.790	90.00	82.05	90.00	97.4168	97.4168	1.4357
Str99	P1	3.703	5.494	14.411	93.079	92.315	104.460	91.9924	91.9924	1.4445

The COMPACK comparison for the predicted low energy crystal structure generated at the 8th, 20th and 99th rank, with the corresponding E_{total} energies –99.01, –97.42 and –91.99 kJ mol^{-1} (called hereafter Str8, Str20 and Str99) respectively show a perfect match with the known experimental polymorphs of pyrazinamide, pyrzin16, pyrzin22 and pyrzin18 (hereafter called δ, α and β, respectively) exhibiting 20 molecules in common within the coordination sphere and a packing *RMSD* value below 1.1 (Fig. 3). The presence of the optimized struc-

tures similar to the experimental polymorphs of pyrazinamide successfully validates the generated landscape. No optimized crystal structures with similar packing to the experimental γ polymorph of pyrazinamide were generated in the landscape, probably because this structure is in a disordered form in the CSD database.

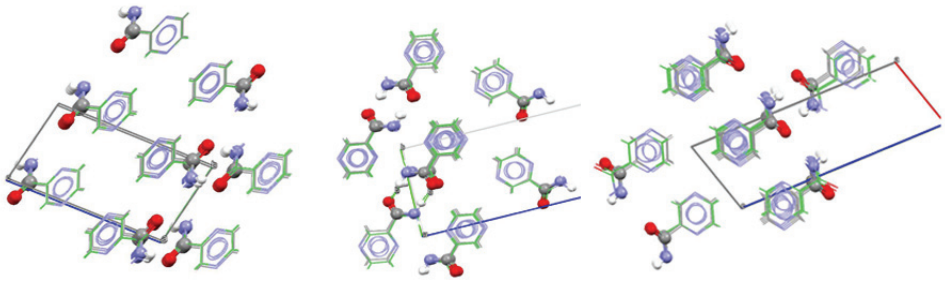

(1) (2) (3)

Fig. 3. Overlay of: 1) Str8 (blue) with the experimental form (green), 2) Str20 (blue) with experimental form (green) and 3) Str99 (blue) with experimental form (green).

TABLE II. Reproduction of the observed crystal structures of pyrazinamide using the experimental conformation (Expminexp) and the matching structures (20 molecules in common) found during the search of the optimized conformations

Conformation	a / Å	b / Å	c / Å	α / °	β / °	γ / °	Density g cm^{-3}	$-E_{total}$ kJ mol^{-1}
Pyrzin16 (δ) observed	5.119	5.705	9.857	97.460	98.170	106.470	–	–
Expminexp	5.194	5.852	9.803	97.924	97.789	110.040	1.5041	99.05
Expminopt	5.852	6.356	13.152	53.749	130.686	129.849	1.504	99.01
Pyrzin22 (α) observed	3.617	6.741	22.463	90.000	92.390	90.000	–	–
Expminexp	3.617	6.714	22.463	90.000	92.395	90.000	1.4354	97.47
Expminopt	3.658	6.898	22.790	90.000	82.050	90.000	1.4357	97.42
Pyrzin18 (β) observed	3.624	10.616	14.315	90.000	101.120	90.000	–	–
Expminexp	14.021	3.791	10.953	90.000	100.402	90.000	1.4280	93.55
Expminopt	3.703	5.494	14.411	93.079	92.315	104.460	1.4445	91.99

The comparative analysis shown in Table II indicates that the optimized hypothetical structures were generated at equivalent total energies with respect to those of the reproduced experimental polymorphs of pyrazinamide, thereby confirming the similarity. As mentioned in the previous report,[21] there was a discrepancy between the β polymorph (Pyrzin 18) at 0 K and its CSP generated equivalent.

Figure 4 shows the powder XRD patterns simulated for both experimental and the corresponding optimized pyrazinamide structures exhibited good match.

The similarity in the patterns confirmed the optimized structures Str8, Str20 and Str99 resemble those of the δ, α and β polymorphs, respectively.

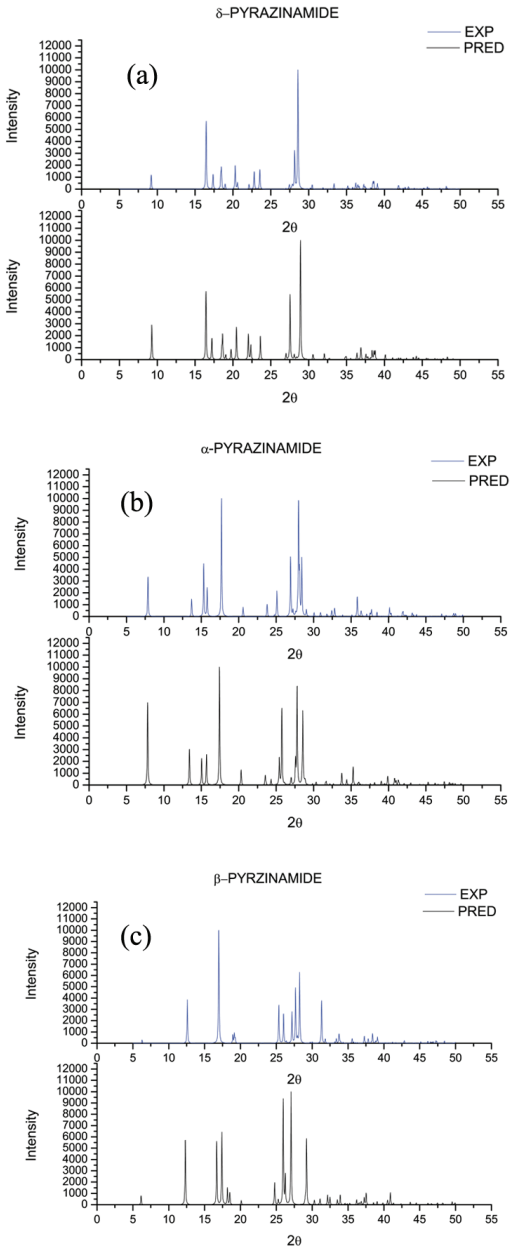

Fig. 4. Comparisons between the simulated XRD patterns of the experimental (top) and predicted (bottom) structures of the a) δ, b) α and c) β polymorphs of pyrazinamide.

Intermolecular short range contacts of rigid molecules are of vital importance to their thermodynamic stability and strong packing. Since the stability of well packed crystal structures is a result of hydrogen bond interactions, the graph sets and key hydrogen bond motifs of the theoretical and experimental crystal structures of pyrazinamide were analysed to explain the structural stability. The analysis demonstrated that the predicted crystal structures Str8, Str20 and Str99 replicate the hydrogen bond interactions of the δ, α and β polymorphs of pyrazinamide. Detailed inspection of the structures showed that the experimental δ and β polymorphs formed a ring type $R_2^2(8)$ hydrogen bond motif, whereas the experimental α polymorph was stabilised by two ring type motifs, $R_2^2(8)$ and $R_2^2(10)$, and three chain type $C_2^2(9)$, $C_2^2(7)$ and $C_2^2(16)$ motifs (Table III). It should be noticed that these ring types are explicitly H-bonded dimers which include N(1) as the donor and N(3)/O(1) as acceptors (N(1)–H(2)···O(1) and N(1)–H(1)···N(3), see Fig. 1 for the atomic numbering); whereas the chain type hydrogen bonds give rise to a zig-zag manner of interaction, with the same donor–acceptor pairs of atoms as for the case of both the experimental and the corresponding predicted α polymorphs. The similarity in the short intermolecular contacts between the experimental and theoretical crystal structures with the same donor acceptor pairs of atoms revealed that Str8, Str20 and Str99 resemble the experimental δ , α and β polymorphs, respectively, with low *RMSD* values (Table III).

TABLE III. List of the common graph sets for the experimental polymorphs and corresponding *ab initio* predicted crystal structures

Conformer label	Hydrogen bond motif	Deviation in E_{total}, kJ mol^{-1}	*RMSD*	Experimental polymorph
Str8	R22(8)	0.0754	0.217	δ
Str20	R22(8) R22(10) C22(7) C22(9) C44(16)	0.0494	0.321	α
Str99	R22(8)	1.5574	1.098	β

From the COMPACK comparison exhibiting the low *RMSD* values and the hydrogen bond motif analysis, it is clear that the predicted crystal structures, Str8, Str20 and Str99, with E_{total} values of –99.01, –97.4 and –91.9 kJ mol^{-1}, respectively, are in good agreement with the δ, α and β polymorphs of pyrazinamide with the same hydrogen bond network that stabilizes the structure. Thermodynamic stability and mechanical strength were analyzed from the C_{ij} matrix,[22] which indicates that the crystal structures met the Born criteria of stability. The estimated mechanical properties of the predicted structures are presented in Table IV.

The results from Table IV revealed that the predicted structures had good matches with the mechanical sensitivity (Young's modulus) of the experimental polymorph of pyrazinamide, which validates the prediction methodology and the potential field used in the current research.

TABLE IV. Comparison of the mechanical properties of the *ab initio* predicted crystal structures and the minimised experimental polymorphs of pyrazinamide

Structure/ Label	Diagonal elements of elastic stiffness tensor matrix, C_{ij}						Young's modulus, GPa
	C_{11}	C_{22}	C_{33}	C_{44}	C_{55}	C_{66}	
δ	42.15949	37.22293	56.43596	12.98786	31.09893	12.31457	34.80518
Str8	32.93377	70.05573	26.60066	26.68087	15.79472	16.98622	34.79503
α	21.3624	48.63952	50.55721	23.50807	8.76284	13.58747	32.05085
Str20	21.2048	48.76925	51.25284	23.87522	8.47534	13.15296	32.06417
β	82.43099	19.57472	40.87375	8.44669	12.50882	16.82628	32.54519
Str99	28.51313	18.95646	99.67113	7.88322	13.27796	8.63193	26.30433

Hirshfeld finger print plot analysis

An investigation of the intermolecular short contacts for the *ab initio* predicted polymorphs of pyrazinamide was performed by analyzing the 2D fingerprint plots for each structure[23] generated using Crystal Explorer.[24] The fingerprint plots for each predicted polymorph showed two distinct spikes at the lower d_i/d_e region indicating the presence of N···H/H···N and O···H/H···O intermolecular short contacts. As the oxygen atom is more electronegative than the nitrogen atom, the interaction was found to be stronger in structures containing O···H/H···O. A comparative analysis of the intermolecular short contacts between the experimental and predicted polymorphs of pyrazinamide revealed the similar nature of the interactions with the N(1) atom at the terminal bond being the donor atom. The 2D fingerprint plots with resolved and unresolved short contacts of the experimental and predicted polymorphs of pyrazinamide are shown in Figs. 5–7.

Figures 5–7 show the 2D finger print plots for the experimental pyrazinamide polymorphs, δ, α and β, together with the corresponding optimized structures, Str8, Str20 and Str99, respectively, with resolved and unresolved short contacts. It could be seen that the structures were stabilized through N···H/H···N and O···H/H···O intermolecular contacts. The former interaction was found to contribute the major percentage to the Hirshfeld surface, indicating its vital importance for both experimental and theoretically predicted structures. It could be observed that the greater electronegativity of the oxygen atom makes the spike more pointed to the low d_i/d_e region for all the experimental and predicted structures, indicating the O···H/H···O interaction.

The interactions contribute ≈18 % for both the experimental δ and α polymorphs, whereas a higher contribution was observed for the experimental β (19.7 %) and Str99 (21.7 %) molecules. The shallow and broad region of the Hirshfeld surface between the spikes indicates weak H···H interactions. The strength and the surface contribution to the Hirshfeld surface for each interaction emphasise the fact that the crystal structures are stabilized through N···H/H···N and O···H/ /H···O intermolecular contacts, whereby, the nitrogen atom is the donor and oxygen is the acceptor.

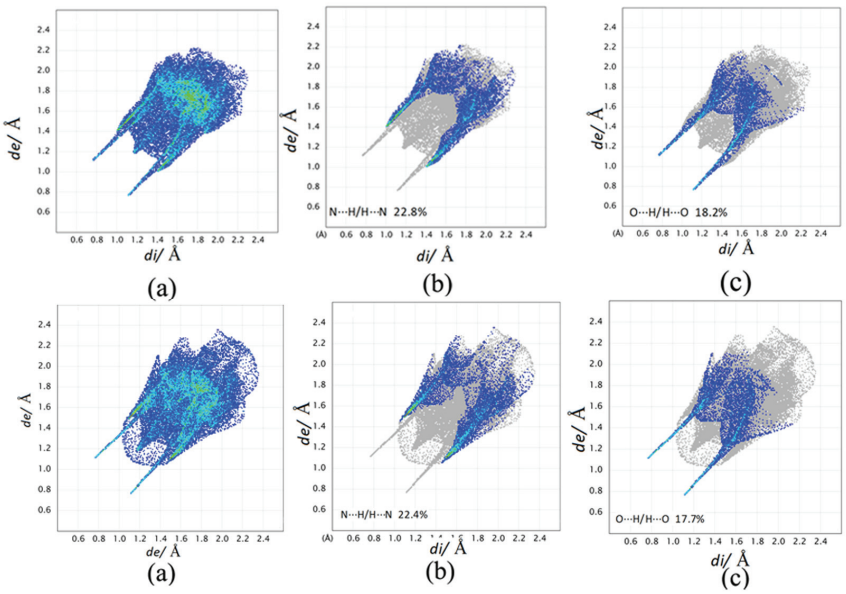

Fig. 5. 2D finger print short contact plots of the experimental δ polymorph (first row) and Str8 (second row) with (a) 100 % contribution of all atoms to the Hirshfeld surface, (b) resolved N···H/H···N interactions and (c) resolved O···H/H···O interactions.

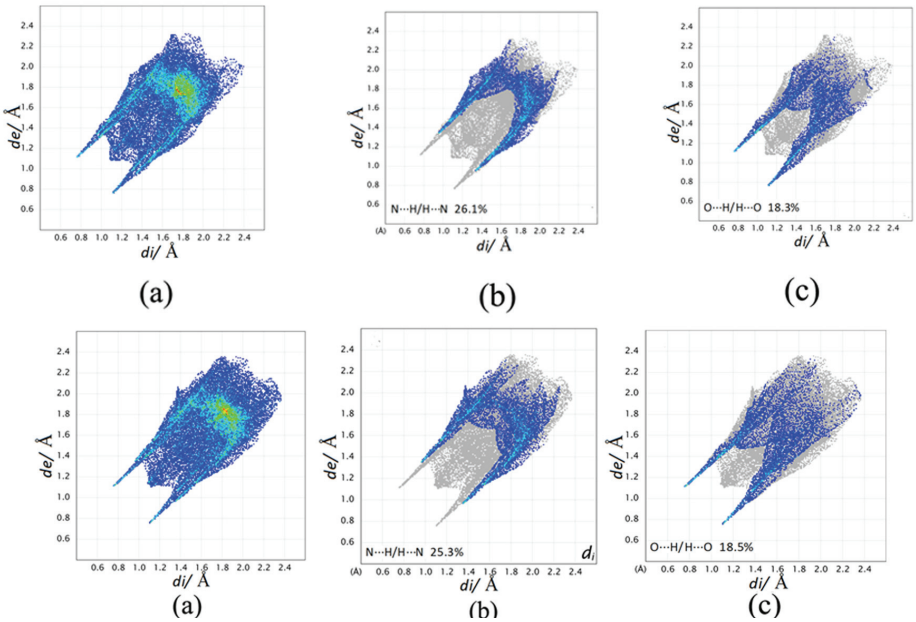

Fig. 6. 2D finger print short contact plots of the experimental α polymorph (first row) and Str20 (second row) with (a) 100 % contribution of all atoms to the Hirshfeld surface, (b) resolved N···H/H···N interactions and (c) resolved O···H/H···O interactions.

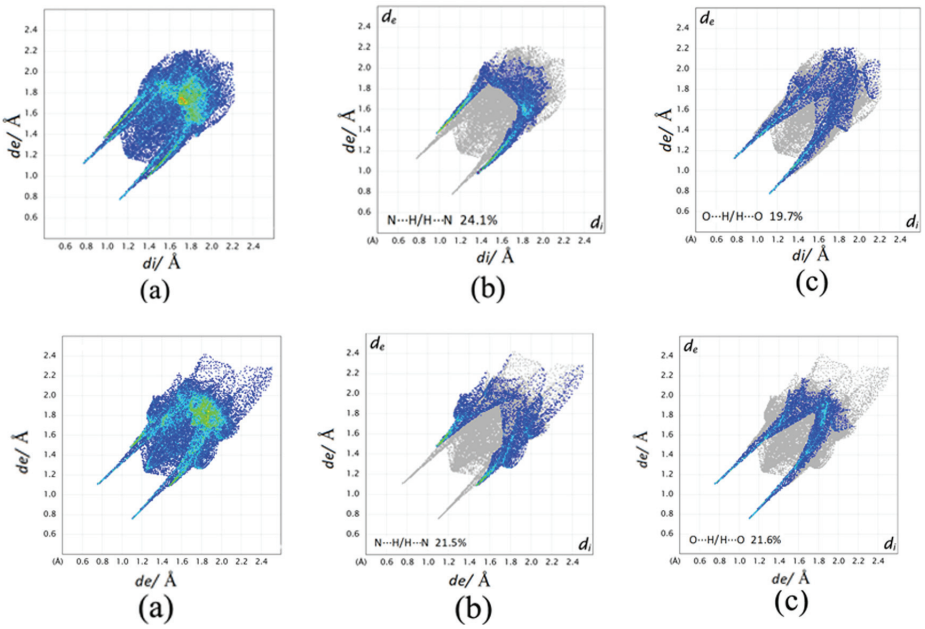

Fig. 7. 2D finger print short contact plots of the experimental β polymorph (first row) and Str99 (second row) with (a) 100 % contribution of all atoms to the Hirshfeld surface, (b) resolved N···H/H···N interactions and (c) resolved O···H/H···O interactions.

The resolved and unresolved contributions of each key interaction with respect to their experimental polymorphs are tabulated in Table V.

TABLE V. The percentage contributions of the key interactions for both experimental and the corresponding theoretical structures

Interaction	exp δ / Str8	exp α / Str20	exp β / Str99
N···H / H···N	22.8 / 22.4	26.1 / 25.3	24.1 / 21.5
O···H / H···O	18.2 / 17.7	18.3 / 18.5	19.7 / 21.6

The data included in Table V show the percentage contribution of the key interactions for both the experimental and their corresponding optimised conformers. An analysis of the data from Table III indicates that the structures called Str8, Str20 and Str99 are the experimental δ, α and β polymorphs of pyrazinamide generated in the energy landscape and thereby justifies the thermodynamic stability of the optimized structures.

CONCLUSIONS

Ab initio crystal structure prediction of the hypothetical densest structures within a flexible conformeric region using a repulsion–dispersion potential field showed good accuracy in predicting the polymorphic structures of pyrazinamide. The energy landscape generated by considering all the likely geometric con-

formers was found to be densely populated. Lattice energy minimisation of the lowest energy structures was performed incorporating the distributed multipole charges. The unique optimized crystal structures were refined and studied thoroughly. The stability of the selected structures was verified by analyzing the intermolecular interactions and second derivative mechanical properties, confirming that the structures had achieved the Born criteria of stability. Detailed analysis of the hydrogen bonds showed that Str8, Str20 and Str99 had similar interactions to the δ, α and β polymorphs of pyrazinamide indicating their physically favourable nature. The Hirshfeld 2D fingerprint plot analysis of the predicted polymorphs revealed that the majority of the interactions are made by the amide and carboxylic group of the molecule, providing a major contribution to the Hirshfeld surface, thereby achieving the stability. The favourable results from the studies made for the theoretical crystal structures of pyrazinamide justify the selected flexible torsion angle and the potential field used for the current prediction methodology. The similarities of the optimized structures with respect to the experimental known polymorphs of pyrazinamide proved the authenticity of the generated energy landscape. Thus the lower energy optimized theoretical structures of pyrazinamide generated *via* the current prediction method in the energy landscape could be considered as potential polymorphs of pyrazinamide, which are resolved or yet to be resolved, thereby the current methodology was validated.

Acknowledgements. The authors are grateful to Dr. Louise S. Price for her kind help and support in using the DMACRYS package software and associated programs, and for assistance in the preparation of this manuscript. The authors are also grateful to DST-SERB for providing financial assistance and support for this research work, carried out under the young scientist fast track project.

ИЗВОД

AB INITIO ПРЕДВИЂАЊЕ ПОЛИМЕРНИХ СТРУКТУРА ПИРАЗИНАМИДА СТУДИЈА ВАЛИДАЦИЈЕ

DAVID STEPHEN [1], P.V. NIDHIN[1] и P. SRINIVASAN[2]

[1]Department of Physics, Sri Shakthi Institute of Engineering and Technology, Coimbatore, India;
[2]Department of Physics, C. Kandaswami Naidu College for Men, Anna Nagar, Chennai, India

Скенирањем површине потенцијалне енергије (PES) добијене оптимизацијом у гасној фази помоћу MP2/6-31G(d,p) методе, урађена је студија валидације за предвиђање могућих стабилних полиморфа пиразинамида у области конформација ниске енергије за флексибилни торзиони угао. Генерисане су хипотетичне кристалне сруктуре са повољном густином паковања за сваки од стабилних конформера које даје PES користећи глобалну претрагу само поља одбојног потенцијала. Најгушће кристалне структуре стабилне енергије су анализиране поузданијом минимизацијом енергије решетке путем дистрибуиране мултиполне анализе користећи репулзионо-дисперзиони потенцијал. Стабилност предсказаних структура са сличним паковањем као и експериментално познати полиморфи пиразинамида, анализирани су испитивањем њихових блиских контаката. Урађена је анализа других извода механичких особина на основу Хесове матрице како би се нагласила термодинамичка стабилност предсказаних полиморфа пиразинамида.

(Примљено 10. децембра 2015, ревидирано 15. марта, прихваћено 7. априла 2016)

REFERENCES

1. M. Vasileiadis, A. V. Kazantsev, P. G. Karamertzanis, C. S. Adjiman, C. C. Pantelides, *Acta Crystallogr., B* **68** (2012) 677
2. D. A. Bardwell, C. S. Adjiman, Y. A. Arnautova, E. Bartashevich, S. X. M. Boerrigter, D. E. Braun, A. J. Cruz-Cabeza, G. M. Day, R. G. Della Valle, G. R. Desiraju, B. P. van Eijck, J. C. Facelli, M. B. Ferraro, D. Grillo, M. Habgood, D. W. M. Hofmann, F. Hofmann, K. V. J. Jose, P. G. Karamertzanis, A. V. Kazantsev, J. Kendrick, L. N. Kuleshova, F. J. J. Leusen, A. V. Maleev, A. J. Misquitta, S. Mohamed, R. J. Needs, M. A. Neumann, D. Nikylov, A. M. Orendt, R. Pal, C. C. Pantelides, C. J. Pickard, L. S. Price, S. L. Price, H. A. Scheraga, J. van de Streek, T. S. Thakur, S. Tiwari, E. Venuti, I. K. Zhitkov, *Acta Crystallogr., B* **67** (2011) 535
3. G. M. Day, *Crystallogr. Rev*. **17** (2011) 3
4. G. Shadeed, *Int. J. Pharm. Pharm. Sci.* **7** (2015) 581
5. Y. Takaki, Y. Sasada, T. Watanabe, *Acta Crystallogr.* **13** (1960) 693
6. G. Ro, H. Sorum, *Acta Crystallogr., B* **28** (1972) 991
7. Y.-H. Luo, Q.-L. Liu, L.-J. Yang, W. Wang, Y. Ling, B.-W. Sun, *Res. Chem. Intermed*. **41** (2015) 7059
8. Gaussian 09, Revision D.1, Gaussian, Inc., Wallingford, CT, USA, 2009
9. J. R. Holden, Z. Du, H. L. Ammon, *J. Comput. Chem*. **14** (1993) 422
10. S. L. Price, M. Leslie, G. W. A. Welch, M. Habgood, L. S. Price, P. G. Karamertzanis, G. M. Day, *Phys. Chem. Chem. Phys.*. **12** (2010) 8478
11. D. E. Williams, S. R. Cox, *Acta Crystallogr. B* **40** (1984) 404
12. D. S. Coombes, S. L. Price, D. J. Willock, M. Leslie, *J. Phys. Chem.* **100** (1996) 7352
13. Z. F. Weng, W. D. S. Motherwell, F. H. Allen, J. M. Cole, *Acta Crystallogr. B* **64** (2008) 348
14. C. Ouvrard, S. L. Price, *Cryst. Growth Des*. **4** (2004) 1119
15. H. Nowell, S. L. Price, *Acta Crystallogr. .B* **61** (2005) 558
16. H. P. G. Thompson, G. M. Day, *Chem. Sci.* **5** (2014) 3173
17. H. L. Ammon, Z. Du, J. R. Holden, L. A. Paquette, *Acta Crystallogr. B* **50** (1994) 216
18. A. J. Stone, GDMA, University of Cambridge, Cambridge, 1999
19. P. P. Ewald, *Ann. Phys. (Berlin, Ger.)* **369** (1921) 253
20. J. A. Chisholm, S. Motherwell, *J. Appl. Crystallogr.* **38** (2005) 228
21. N. Wahlberg, P. Ciochon, V. Petrick, A. O. Madsen, *Cryst. Growth Des.* **14** (2014) 381
22. A. T. Anghel, G. M. Day, S. L. Price, *CrystEngComm* **4** (2002) 348
23. S. Madan Kumar, B. C. Manjunath, G. S. Lingaraju, M. M. M. Abdoh, M. P. Sadasiva, N. K. Lokanath, *Cryst. Struct. Theory Appl.* **2** (2013) 124
24. M. A. Spackman, J. J. McKinnon, *CrystEngComm* **4** (2002) 378.